

RESEARCH

Open Access



Early introduction of IL-10 weakens BCG revaccination's protection by suppressing CD4⁺Th1 cell responses

Qing Lei^{1†}, Hui Fu^{1†}, Zongjie Yao^{1†}, Zijie Zhou^{1,2}, Yueqing Wang³, Xiaosong Lin¹, Yin Yuan⁴, Qi Ouyang¹, Xinyue Xu¹, Jinge Cao¹, Mengze Gan¹ and Xionglin Fan^{1*} 

Abstract

Background The Bacillus Calmette-Guérin (BCG) vaccine, currently the sole authorized vaccine against tuberculosis (TB), demonstrates limited effectiveness in safeguarding adolescents and adults from active TB, even when administered as a booster with either BCG itself or heterologous vaccine candidates. To effectively control the persistent epidemic of adult TB, it is imperative to investigate the mechanisms responsible for the suboptimal efficacy of the BCG prime-boosting strategy against primary *Mycobacterium tuberculosis* (*M.tb*) infection.

Methods C57BL/6J mice were immunized with the BCG vaccine either once or twice, followed by analysis of lung tissue to assess changes in cytokine levels. Additionally, varying intervals between vaccinations and detection times were examined to study IL-10 expression across different organs. IL-10-expressing cells in the lungs, spleen, and lymph nodes were analyzed through FACS and intracellular cytokine staining (ICS). BCG-revaccinated *IL-10*^{-/-} mutant mice were compared with wild-type mice to evaluate antigen-specific IgG antibody and T cell responses. Protection against *M.tb* aerosol challenge was evaluated in BCG-revaccinated mice, either untreated or treated with anti-IL-10R monoclonal antibody.

Results IL-10 was significantly upregulated in the lungs of BCG-revaccinated mice shortly after the booster immunization. IL-10 expression peaked in the lungs 3–6 weeks post-revaccination and was also detected in lymph nodes and spleen as early as 2 weeks following the booster dose, regardless of the intervals between the prime and booster vaccinations. The primary sources of IL-10 in these tissues were identified as macrophages and dendritic cells. Blocking IL-10 signaling in BCG-revaccinated mice—either by using *IL-10*^{-/-} mutant mice or administering anti-IL-10R monoclonal antibody increased levels of antigen-specific IFN- γ ⁺ or IL-2⁺ CD4⁺ T cells, enhanced central and effector memory CD4⁺ T cell responses, and provided better protection against aerosol infection with 300 CFUs of *M.tb*.

Conclusion Our findings are crucial for formulating effective immunization strategies related to the BCG vaccine and for developing efficacious adult TB vaccines.

[†]Qing Lei, Hui Fu and Zongjie Yao contributed equally to this work.

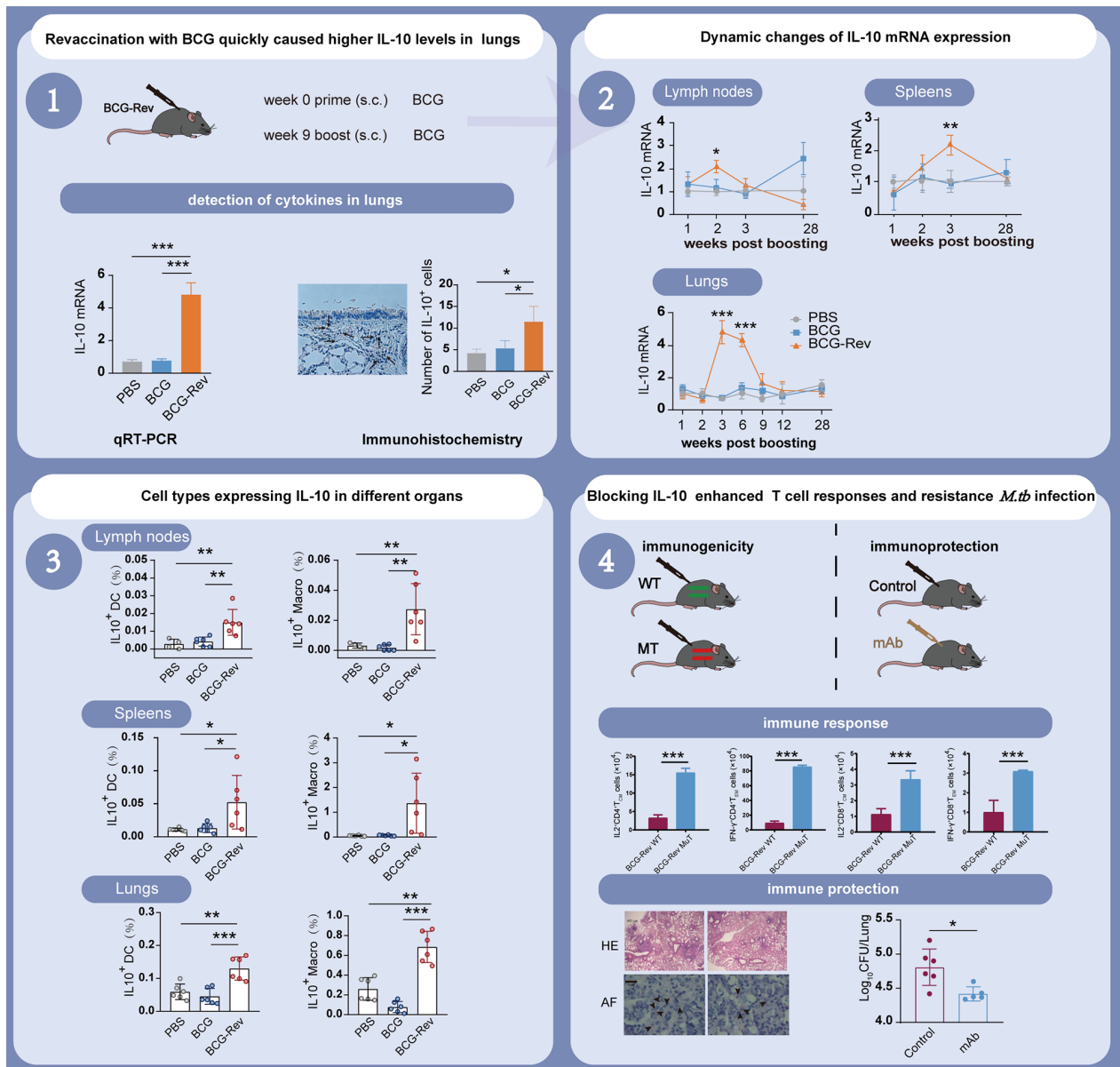
*Correspondence:
Xionglin Fan
xlfan@hust.edu.cn

Full list of author information is available at the end of the article



© The Author(s) 2024. **Open Access** This article is licensed under a Creative Commons Attribution-NonCommercial-NoDerivatives 4.0 International License, which permits any non-commercial use, sharing, distribution and reproduction in any medium or format, as long as you give appropriate credit to the original author(s) and the source, provide a link to the Creative Commons licence, and indicate if you modified the licensed material. You do not have permission under this licence to share adapted material derived from this article or parts of it. The images or other third party material in this article are included in the article's Creative Commons licence, unless indicated otherwise in a credit line to the material. If material is not included in the article's Creative Commons licence and your intended use is not permitted by statutory regulation or exceeds the permitted use, you will need to obtain permission directly from the copyright holder. To view a copy of this licence, visit <http://creativecommons.org/licenses/by-nc-nd/4.0/>.

Graphical abstract



Keywords BCG revaccination, BCG prime-boost strategy, Adult tuberculosis, Primary *Mycobacterium tuberculosis* infection, IL-10 inhibition, Memory CD4⁺ T cell

Introduction

The Bacillus Calmette-Guérin (BCG) vaccine, derived from the attenuated virulent strain of *Mycobacterium bovis*, has remained the only vaccine approved for tuberculosis (TB) prevention for over a century [1]. The World Health Organization (WHO) has recommended the inclusion of the BCG vaccine in expanded immunization programs since 1974 [2]. Currently, 156 countries implement the BCG vaccine, each following specific national

guidelines [3, 4]. Neonatal BCG vaccination has been widely adopted in over 80% of these countries, with an average coverage rate exceeding 90%. Despite ongoing efforts to curb its spread, TB continues to pose a significant threat to global public health [5]. In 2022, 10.6 million new TB cases were reported globally, with 1.3 million deaths, and adolescents and adults accounted for approximately 90% of these new cases [6]. Moreover, around 25% of the global population carries latent tuberculosis

infection (LTBI), with 5–10% progressing to active TB over their lifetimes [5, 7]. Therefore, neonatal BCG vaccination is insufficient in preventing active TB or LTBI during adolescence and adulthood [8]. Consequently, there is an urgent need to develop more efficacious vaccines or immunization strategies to better control TB in adults.

Developing more efficacious TB vaccine candidates remains a significant challenge, especially as almost no candidates have demonstrated stronger protection than the current BCG immunization in preclinical and clinical trials. Consequently, replacing or eliminating the existing BCG immunization regimen for infants is impractical [1, 9]. To enhance the efficacy of the BCG vaccine in preventing adult TB, prioritizing BCG revaccination is considered a promising strategy due to its convenience and simplicity. Prior to 2019, 78 countries, including China, recommended administering the BCG vaccine on two or more separate occasions at different intervals, based on historical data [3, 4]. As of 2019, seven countries have continued to include booster doses of the BCG vaccine in their national guidelines [3, 4]. Nevertheless, the WHO has not endorsed the BCG revaccination strategy [10, 11]. To overcome these obstacles, an alternative approach involving BCG prime-heterologous boosting regimens has seen rapid development [12, 13]. Unfortunately, nearly half of the heterologous boosting vaccine candidates [12, 13], particularly those undergoing clinical trials [14], have failed to demonstrate improved efficacy in BCG-primed animal models against primary *Mycobacterium tuberculosis* (*M.tb*) infection in preclinical studies. Recent findings from a phase 2b clinical trial further support the conclusion that the efficacy of BCG revaccination in adults against primary *M.tb* infection is below 50% [15]. Notably, our previous study has demonstrated that BCG primed mice and then either revaccinated with BCG [16] or heterologous boosted with subunit protein CMFO vaccine are effective approaches for preventing and controlling LTBI rather than primary *M.tb* infection [17], attributing to upregulated IL-2 positive central memory T (T_{CM}) and IFN- γ^+ effector memory T (T_{EM}) cell responses following the booster inoculation [16]. However, the underlying mechanisms contributing to the suboptimal efficacy of BCG revaccination or heterologous boosters in primary *M.tb* infection remain unclear.

The cellular immune response mediated by Th1 cells is widely recognized as crucial in defending against TB infection [18–20]. A central question in this field is whether BCG revaccination or other heterologous booster vaccines may affect T cell function. To explore this question, animal models were established by immunizing both wild-type (WT) and mutant-type (MT) mice with the BCG vaccine either once or twice. Subsequently, the lung tissue of the immunized mice was analyzed using qRT-PCR and immunohistochemistry to identify

cytokines with altered expression levels. The anti-inflammatory cytokine IL-10 was the only one significantly upregulated shortly after BCG booster immunization. Further analysis of the temporal and spatial expression profiles of IL-10 was conducted in this study to investigate its role in modulating T cell responses and preventing primary *M.tb* infection in BCG-revaccinated mice. Our findings are crucial for improving adult TB control through enhanced BCG immunization strategies or the development of novel vaccine candidates.

Materials and methods

Mice

This study utilized specific pathogen-free female C57BL/6J mice, aged 6–8 weeks, sourced from Charles River (Beijing, China). Mutant type (MT) C57BL/6J mice with the *IL-10* gene (*IL-10^{-/-}*) knocked out, were generously provided by Prof. Xiaolian Zhang of Wuhan University. Both groups of mice were housed at the Animal Experimental Center, Tongji Medical College, Huazhong University of Science and Technology.

Ethics statement

All animal experiments were conducted in accordance with the ethical guidelines and procedures approved by the Committee on the Ethics of Animal Experiments at Tongji Medical College (IACUC Number: 3538).

Immunization and antibody treatment

The BCG vaccine (China strain) was cultured on Middlebrook 7H11 agar plates at 37 °C. Mice were subcutaneously (s.c.) immunized with 10^6 CFU of the BCG vaccine for the first dose, followed by a booster dose administered at varying intervals during the experiments. Mice treated with PBS or a single dose of the BCG vaccine were used as controls. The monoclonal antibody (mAb) targeting mouse IL-10R (BioXCell, West Lebanon, USA) was administered intraperitoneally (i.p.) to inhibit IL-10 signaling as required. Mice in each group were euthanized in the designated euthanasia room by gradually inflating a carbon dioxide (CO₂) compressed gas cylinder, after which follow-up analyses were performed. All experiments were conducted in triplicate.

Different cytokines mRNAs detected by qRT-PCR

Quantitative real-time PCR (qRT-PCR) was used to assess the expression levels of various cytokines in lung tissues, including IFN- γ , TNF- α , IL-17 A, TGF- β , IL-10, IL-1 β , IL-6, IL-2, and IL-4. Briefly, total RNA was extracted from the tissues using TRIzol reagent (Invitrogen, Carlsbad, USA) and reverse-transcribed into cDNA using the ReverTra Ace qPCR RT Kit (TOYOBO, Osaka, Japan) according to the manufacturer's instructions. Primer sequences for the experiments are provided in

Supplementary Table 1. qRT-PCR experiments were conducted using the Bio-Rad CFX96 machine and the SYBR Green Realtime PCR Master Mix reagent (Thermo Scientific, Waltham, USA). The $2^{-\Delta\Delta Ct}$ method was used to quantify relative mRNA expression levels, with GAPDH mRNA serving as the control. The $\Delta\Delta Ct$ was calculated by subtracting the experimental ($Ct_{\text{cytokine}} - Ct_{\text{GAPDH}}$) value from the control ($Ct_{\text{cytokine}} - Ct_{\text{GAPDH}}$) value. Results are expressed as the mean \pm standard deviation (SD).

Detection of IL-10 expression in lung tissues through immunohistochemistry

Lung tissue from each euthanized mouse was fixed in 4% formalin, sectioned, and analyzed immunohistochemically for IL-10 protein expression using anti-IL-10 antibodies (Servicebio, Wuhan, China) and an HRP-conjugated secondary antibody. IL-10 expression was visualized using a diaminobenzidine substrate and hematoxylin counterstaining. Eight fields of view were examined under a light microscope at 400 \times magnification, and the number of cells exhibiting a brownish-yellow color was counted. Results are presented as the mean \pm standard deviation (SD).

FACS and intracellular cytokine staining (ICS) for the detection of IL-10 positive cells

A total of 2×10^6 cells, isolated from the spleen, lung, or inguinal lymph nodes of each mouse, were seeded into individual wells of 96-well plates and incubated for 6 h with a cell activation cocktail containing Brefeldin (Cat#423304, Biolegend, Santiago, USA). After washing with ice-cold PBS, the cells were incubated with anti-rat CD16/CD32 antibody (Cat#553141, BD, USA) at 4 $^{\circ}\text{C}$ for 15 min. Dead cells were stained using fixable viability stain 620 (Cat#564996, BD, USA) and the staining was stopped with PBS containing 5% FBS. Cells were then stained with various surface markers, including anti-CD25-PE-CY7 (Cat#561780), anti-CD11c-BV650 (Cat#561241), anti-CD8-BV510 (Cat#563068), anti-F4/80-BV421 (Cat#565411), anti-CD4-APC-CY7 (Cat#552051), anti-B220-BV605 (Cat#3554467), and anti-CD3-FITC (Cat#553061), as well as intracellular markers such as anti-IFN- γ -PE-CY7 (Cat#557649), anti-IL17A-APC (Cat#560184), anti-Foxp3-APC (Cat#560401), and anti-IL-10-PE (Cat#563708) antibodies, all obtained from BD, USA. The proportions of IL-10 positive DC (CD11c $^{+}$), macrophages (F4/80 $^{+}$), B cells (B220 $^{+}$), T cells (CD3 $^{+}$), Th cells (CD3 $^{+}$ CD4 $^{+}$), Th1 cells (CD3 $^{+}$ CD4 $^{+}$ IFN- γ $^{+}$), Th17 cells (CD3 $^{+}$ CD4 $^{+}$ IL17A $^{+}$), Tc cells (CD3 $^{+}$ CD8 $^{+}$), and Treg cells (CD25 $^{+}$ Foxp3 $^{+}$) in each organ were determined using FlowJo software and an LSRII multicolor flow cytometer from BD Biosciences. Results are presented as mean \pm standard deviation (SD).

Detection of CMFO-specific T cells by ICS and FACS

Our laboratory previously constructed the plasmid pET30b-CMFO and confirmed its stable expression in *E. coli* BL21 (DE3) [17]. The CMFO fusion protein comprises four proteins: Rv2875, Rv3044, Rv2073c, and Rv0577, and is capable of inducing high levels of antigen-specific T cells and providing robust anti-*M. tuberculosis* (*M.tb*) immune protection in mouse models [17, 21, 22]. The CMFO fusion proteins were prepared using the same procedure as described previously [17]. BCG-revaccinated wild-type and *IL-10* $^{-/-}$ C57BL/6J mice were employed as experimental models to identify CMFO-specific T cells using intracellular cytokine staining (ICS) and fluorescence-activated cell sorting (FACS), as previously described [16]. Briefly, 5×10^6 splenocytes or lung cells from each mouse were incubated with 20 μg CMFO and 1 μg anti-mouse CD28 antibody (Cat#102116, Biolegend, USA) for 4 h, followed by the addition of 2 μM monensin solution (Cat#420701, Biolegend, USA) for 12 h. Dead cells were excluded using Fixable Viability Stain 450 (Cat#562247, BD, USA). Cells were then stained with surface and intracellular biomarkers from BD, including anti-CD44-FITC (Cat#561859), anti-CD62L-PerCP-Cy5.5 (Cat#560513), anti-CD4-APC-Cy7 (Cat#552051), anti-CD8a-BV510 (Cat#563068), anti-IL-2-APC (Cat#554429), and anti-IFN- γ -PE (Cat#557649). The absolute numbers of CMFO-specific IFN- γ $^{+}$ or IL-2 $^{+}$ T cells, effector memory T cells ($T_{\text{EM}}^{\text{CD62L}^{\text{lo}} \text{CD44}^{\text{hi}}}$), and central memory T cells ($T_{\text{CM}}^{\text{CD62L}^{\text{hi}} \text{CD44}^{\text{hi}}}$) in each organ were determined using FlowJo software. Results are presented as mean \pm standard deviation (SD).

Detection of CMFO specific cytokines secreted by splenocytes using CBA method

Five million (5×10^6) splenocytes from each mouse were stimulated with 20 μg CMFO and 1 μg anti-mouse CD28 (Cat#102116, Biolegend) for 72 h. Cytokines secreted by splenocytes in culture supernatants, such as IFN- γ , TNF- α , IL-6, IL-17 A, IL-2, IL-4, and IL-10, were quantified using mouse Th1/Th2/Th17/Treg cytokine kits (Cat#LX-560485, BD, USA). Results are presented as mean \pm standard deviation (SD) for each group.

ELISA detection of CMFO-specific IgG and subclass

IgG (Cat#151276, Abcam, USA), IgG2a (Cat#157720), and IgG1 (Cat#133045) antibodies were utilized to detect CMFO-specific endpoint titers in serum samples from individual mice via ELISA, as described previously [17]. Antibody titers for each mouse were calculated as \log_{10} (endpoint titer), and results are presented as mean \pm standard error of the mean (SEM) for each group.

Evaluation of the protective effect against virulent *M. Tuberculosis* H37Rv infection

Mice were infected with virulent *M. tuberculosis* H37Rv via aerosol exposure (Jingnuo Biotech., Shanghai, China) and subsequently housed in an ABSL-3 laboratory. The day following infection, five non-immunized mice were euthanized, and their lungs were aseptically extracted to quantify colony-forming units (CFUs) and determine the actual infection dose. Four weeks post-infection, protection levels were assessed as previously described [17]. Briefly, lung tissue homogenates from each infected mouse were prepared, serially diluted, and then plated on Middlebrook 7H11 agar. After incubation for 3–4 weeks at 37 °C, CFUs were enumerated, and results are presented as the mean \log_{10} (CFU) \pm standard error of the mean (SEM). Additionally, lung tissue samples were stained using either hematoxylin and eosin (HE) or acid-fast (AF) stains.

Statistical analyses

Data were collected and analyzed using GraphPad Prism 9. Statistical significance was determined using a *p*-value threshold of 0.05 with either a two-tailed Student's *t*-test or one-way ANOVA, as appropriate.

Results

Revaccination with BCG quickly causes higher IL-10 levels in the lungs

The immunomodulatory effects of cytokines significantly influence immunity and infection [23]. To identify anti-inflammatory cytokines affecting the protective efficacy of BCG revaccination, C57BL/6J mice were initially immunized subcutaneously (*s.c.*) with 10^6 CFU of BCG, followed by a booster dose nine weeks later (BCG revaccination group). Control mice were treated with PBS or immunized with the BCG vaccine once. Three weeks later, the mRNA expression levels of different cytokines in the lung tissues of mice were assessed using qRT-PCR (Fig. 1A). Although mRNA levels of TNF- α , IFN- γ , IL-2, IL-6, TGF- β , IL-4, and IL-1 β were consistent across all groups, the BCG revaccination group significantly induced higher levels of IL-10 and IL-17 A compared to the PBS and BCG groups (Fig. 1B). Immunohistochemical analysis further revealed increased IL-10 protein expression in lung tissues following BCG revaccination (Fig. 1C-D). These results indicate that IL-10, a cytokine with anti-inflammatory properties, is rapidly elevated in lung tissues following re-inoculation with the BCG vaccine.

IL-10's lung expression peaks 3–6 weeks post BCG revaccination

To further investigate the effect of the interval duration between priming and subsequent boost immunization

on IL-10 expression in the lung, BCG-primed mice were administered a second dose of the BCG vaccine at 5, 9, or 14 weeks, respectively. Three weeks after the booster immunization, IL-10 expression in lung tissues was analyzed using qRT-PCR (Fig. 2A). Notably, BCG-revaccinated mice exhibited higher IL-10 levels in lung tissues, regardless of the interval duration, compared to control groups receiving either PBS or BCG alone (Fig. 2B). Additionally, IL-10 expression patterns in the lung were assessed after a 9-week interval between the priming and booster vaccinations to explore the impact of detection time (1, 2, 3, 6, 9, 12, and 28 weeks) following the boost inoculation (Fig. 2C). Interestingly, IL-10 mRNA levels in the lungs were significantly elevated at weeks 3 and 6 post-BCG revaccination, with no significant differences among the groups at other time points (Fig. 2D-E). Therefore, IL-10 expression in the lungs peaks three to six weeks after the second dose of repeated BCG immunization and is unaffected by the interval between doses.

IL-10 is quickly induced in mouse lymph nodes and spleen via macrophages and DCs following BCG revaccination

Mice were subcutaneously immunized with the BCG vaccine at week 0 and 9. IL-10 expression in peripheral immune organs, including lymph nodes and spleen, was measured using qRT-PCR at week 1, 2, 3, and 28 after the booster dose (Fig. 3A). No statistically significant difference was observed in IL-10 mRNA levels between the BCG group and the PBS group in lymph nodes and spleen at different time points. Notably, IL-10 mRNA levels were significantly higher in the BCG revaccination group at week 2 and 3 after the booster dose compared to both PBS and BCG groups (Fig. 3B-E). ICS and FACS analyses were conducted to identify specific cell types responsible for IL-10 production following repeated BCG immunization, including B cells, dendritic cells (DCs), macrophages, T cells, and T cell subsets such as Th1, Th17, helper (Th), cytotoxic (Tc), and regulatory T cells (Treg) (Fig. 4A, Supplementary Fig. 1). Two weeks after the second dose, mice that received the BCG vaccine exhibited a higher number of IL-10⁺ DCs, IL-10⁺ macrophages, and IL-10⁺ B cells in the lymph nodes compared to PBS and BCG control groups (Fig. 4B). Three weeks after the booster dose, BCG revaccinated mice exhibited a significant increase in IL-10⁺ DCs and IL-10⁺ macrophages in the spleen and lung, as well as IL-10⁺ B cells in the spleen (Fig. 4C-D). Additionally, compared to the PBS control group, BCG-revaccinated mice exhibited a significant increase in the number of IL-10⁺ T, Th, and Th1 cells in the spleens (Fig. 4C). These results suggest that macrophages and dendritic cells in the lymph nodes and spleen are the primary sources of IL-10 production shortly after BCG revaccination.

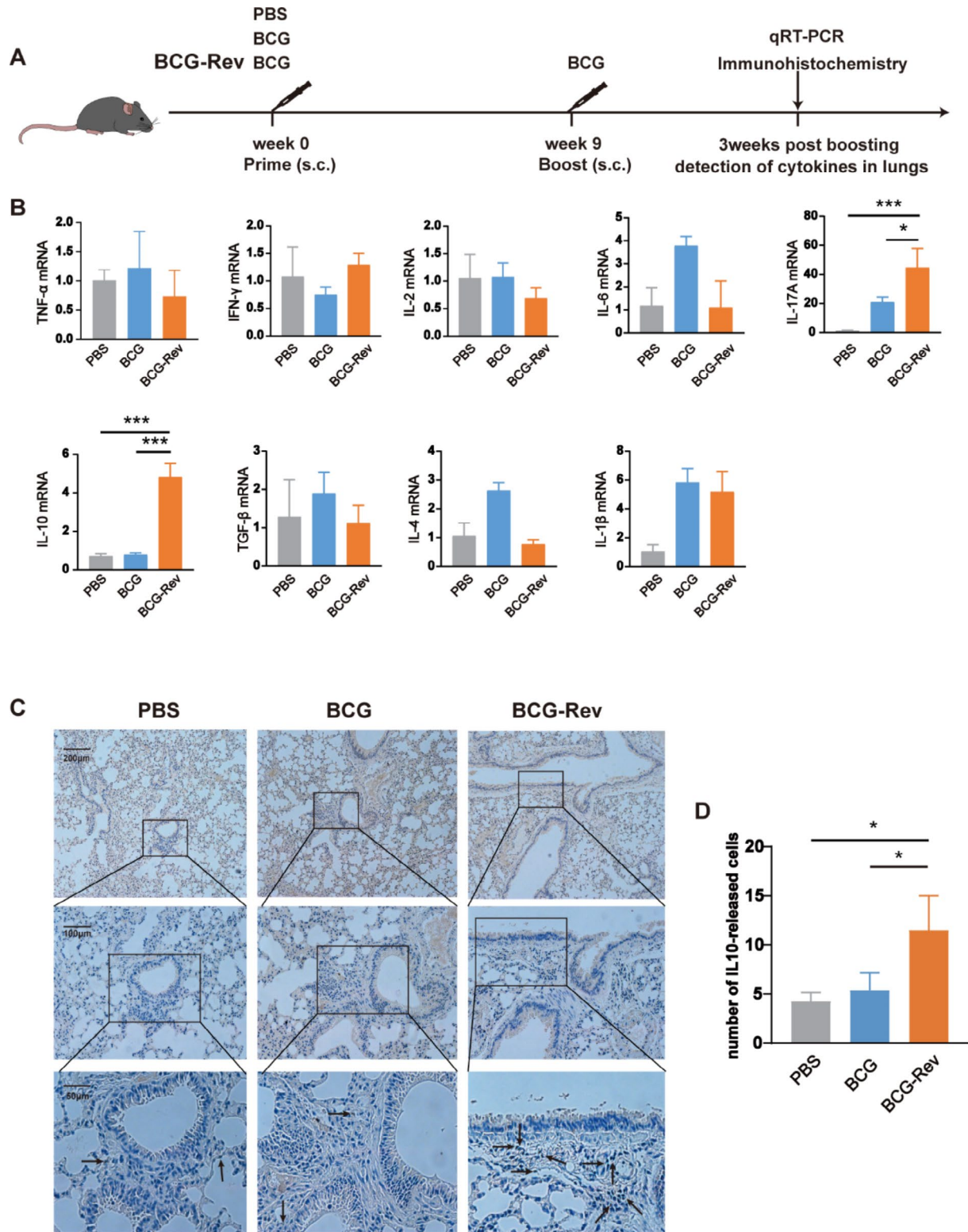


Fig. 1 IL-10 expression in lung tissues of vaccinated mice ($n = 3$). C57BL/6J mice were primed with 10^6 CFU of BCG and received a booster dose at week 0 and 9 (designated as BCG-rev). Three weeks post-immunization, qRT-PCR and immunohistochemistry were employed to assess cytokine expression. PBS and BCG were used as controls. **(A)** Immunization and detection schedule. **(B)** Comparison of mRNA expression levels of cytokines—TNF- α , IFN- γ , IL-2, IL-6, IL-17A, IL-10, TGF- β , IL-4, and IL-1 β —in the lungs among three groups by qRT-PCR. **(C)** Immunohistochemical images displaying IL-10 expression. **(D)** Quantitative analysis of immunohistochemical results, expressed as mean \pm SD ($n = 3$). * $P < 0.05$; ** $P < 0.01$; *** $P < 0.001$

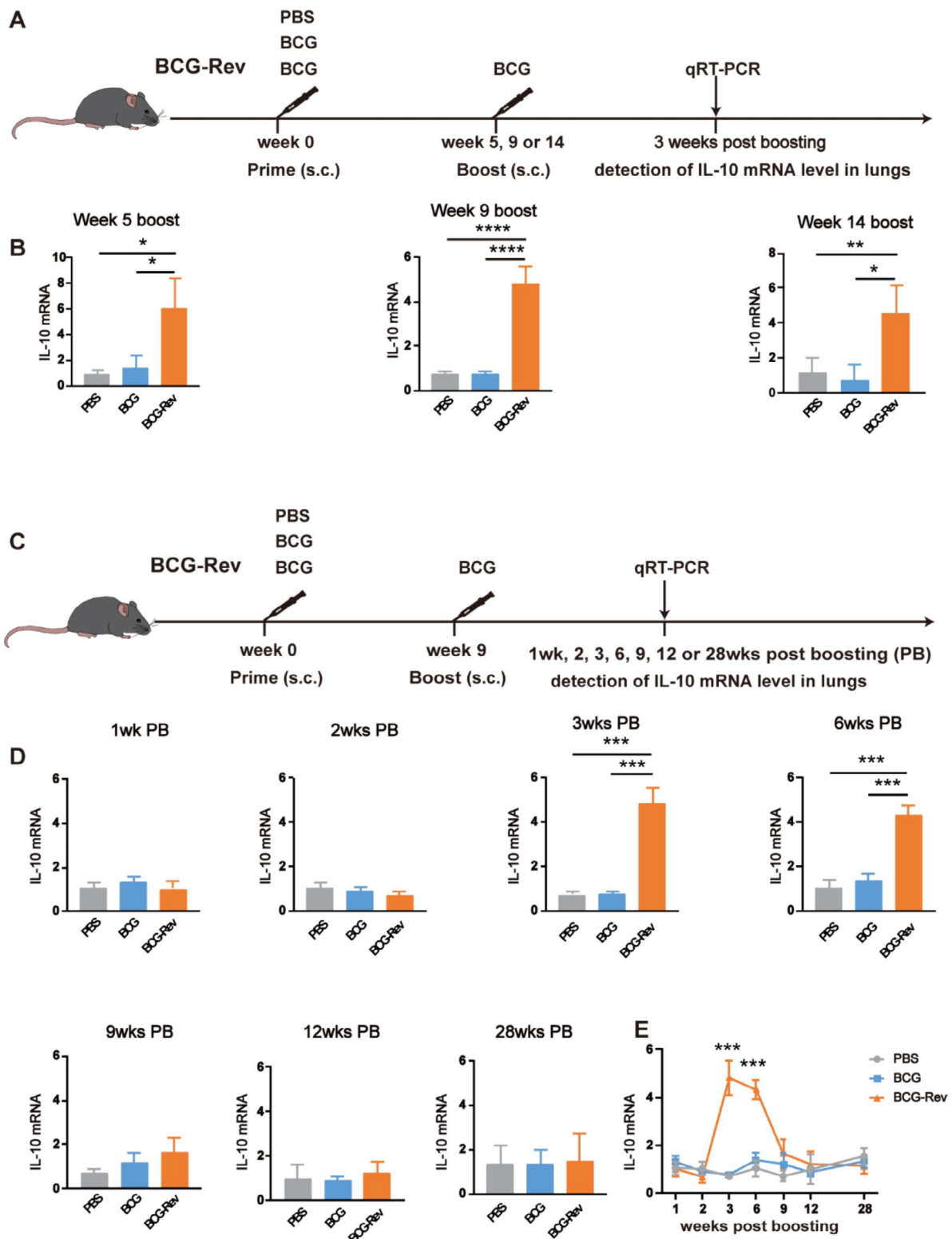


Fig. 2 The factors influencing IL-10 expression in lung tissues ($n=3$). BCG-primed C57BL/6J mice received a secondary BCG vaccine dose at week 5, 9, or 14. Three weeks post-boost immunization, IL-10 expression in lung tissues was quantified via qRT-PCR. **(A)** Immunization and detection schedule. **(B)** IL-10 mRNA levels were compared across groups with varying interval times. Alternatively, C57BL/6J models were revaccinated with the BCG vaccine at a 9-week interval to assess IL-10 expression in the lungs at multiple time points (1, 2, 3, 6, 9, 12, and 28 weeks) post-booster vaccination. **(C)** Schedule of immunization and detection. **(D)** Comparison of IL-10 mRNA levels at different time points following boost immunization. **(E)** Dynamic changes in IL-10 mRNA expression in the lung. Results are presented as mean \pm SD ($n=3$). * $P < 0.05$; ** $P < 0.01$; *** $P < 0.001$

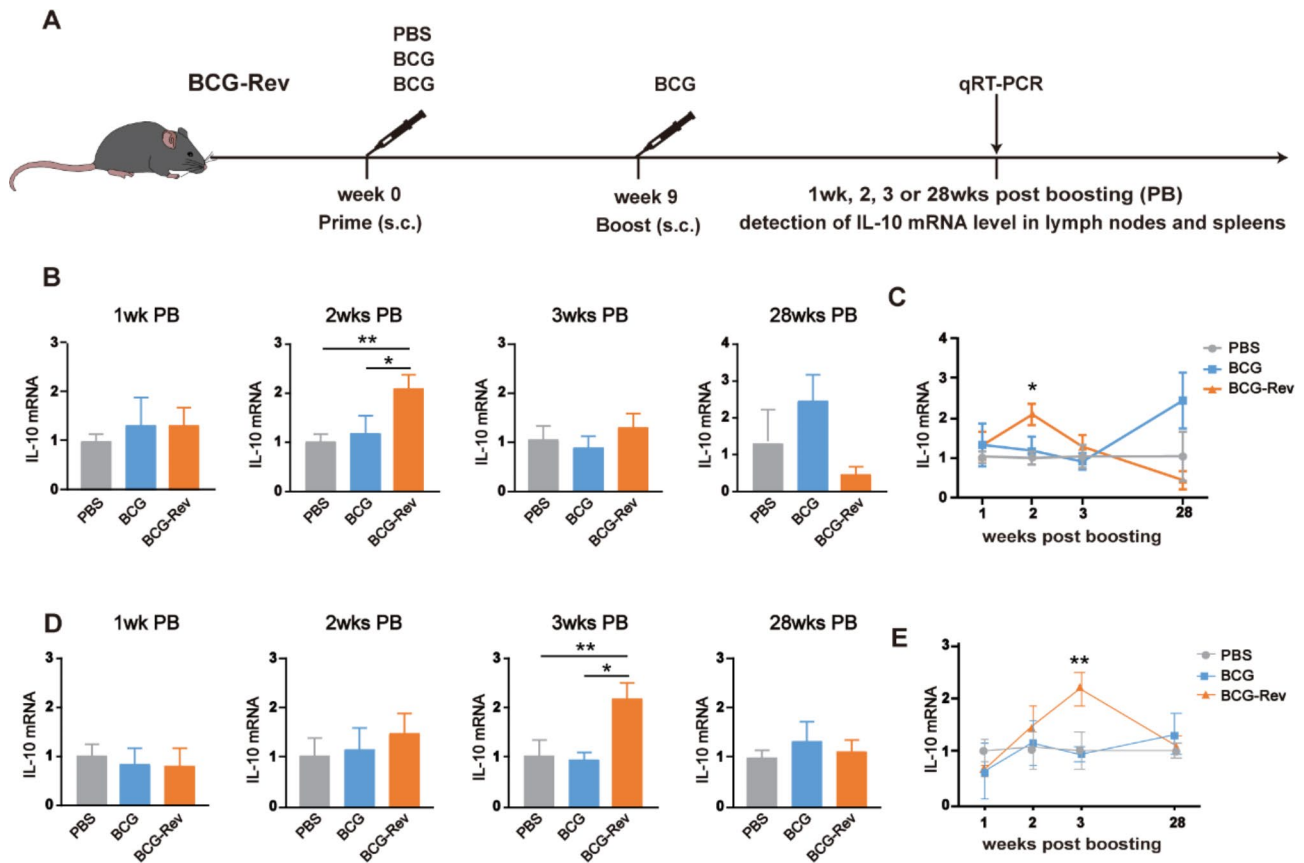


Fig. 3 Dynamic changes of IL-10 mRNA expression in lymph nodes and spleens throughout the duration of detection ($n=3$). **(A)** Immunization and detection schedule. C57BL/6J mice received the BCG vaccine at week 0 and 9. qRT-PCR was performed at week 1, 2, 3, and 28 post-booster to evaluate IL-10 mRNA expression in lymph nodes and spleen. **(B)** Comparative analysis of IL-10 mRNA expression in lymph nodes across different time points. **(C)** Temporal dynamics of IL-10 mRNA expression in lymph nodes throughout the detection period. **(D)** Comparative analysis of IL-10 mRNA expression in the spleen at various time points. **(E)** Temporal dynamics of IL-10 mRNA expression in the spleen. Results were presented as mean \pm SD. * $P < 0.05$; ** $P < 0.01$; *** $P < 0.001$

IL-10 knockout mice enhanced antigen-specific T cell responses following BCG revaccination compared to wild-type mice

The influence of IL-10 on T cell responses in BCG-revaccinated mice was further investigated. Six- to eight-week-old WT and *IL-10*^{-/-} mice were subcutaneously immunized with the BCG vaccine at week 0 and 9. Three weeks after the second dose, the numbers of CMFO-specific T cells in the spleen and lung of vaccinated mice were quantified by ICS and FACS (Fig. 5A, Supplementary Fig. 2). In comparison to the WT group, BCG revaccinated *IL-10*^{-/-} mice exhibited higher levels of IFN- γ ⁺ CD4⁺ T cells, IFN- γ ⁺ CD4⁺ T_{EM} cells, and IL-2⁺ CD4⁺ T_{CM} cells in the both spleen (Fig. 5B) and lung (Fig. 5C), as well as IL-2⁺ CD4⁺ T cells in the spleen. Moreover, upon CMFO stimulation, BCG-revaccinated *IL-10*^{-/-} mice showed elevated levels of IL-2, IFN- γ , TNF- α , IL-17A, and IL-6 in the splenocytes supernatant compared to WT mice (Fig. 5D). Additionally, both BCG revaccinated *IL-10*^{-/-} and WT mice produced similar levels of CMFO-specific IgG, IgG2a, and IgG1 in the serum

(Supplementary Fig. 3A-C), and IgG2a/IgG1 ratios was comparable between both groups (Supplementary Fig. 3D). Therefore, BCG-revaccinated *IL-10*^{-/-} mice enhance antigen-specific CD4⁺ T cells, particularly memory CD4⁺ T cell responses in comparison to the WT mice.

Blocking IL-10 signaling enhances BCG-revaccinated mice’s resistance to primary *M.tb* infection

To investigate the role of IL-10 in the protective efficacy of BCG revaccination, mice were subcutaneously immunized with the BCG vaccine at week 0 and 9. IL-10 signaling was blocked by intraperitoneal administration of anti-IL-10R antibodies one day before the booster dose, followed by weekly injections leading up to the challenge with virulent *M.tb*. At week twelve, mice were challenged with 300 CFU *M. tuberculosis* H37Rv via aerosol exposure. Four weeks later, the lungs of each mouse were aseptically harvested to assess protective efficacy (Fig. 6A). BCG-revaccinated mice treated with IL-10R mAb exhibited significantly lower bacterial loads in the

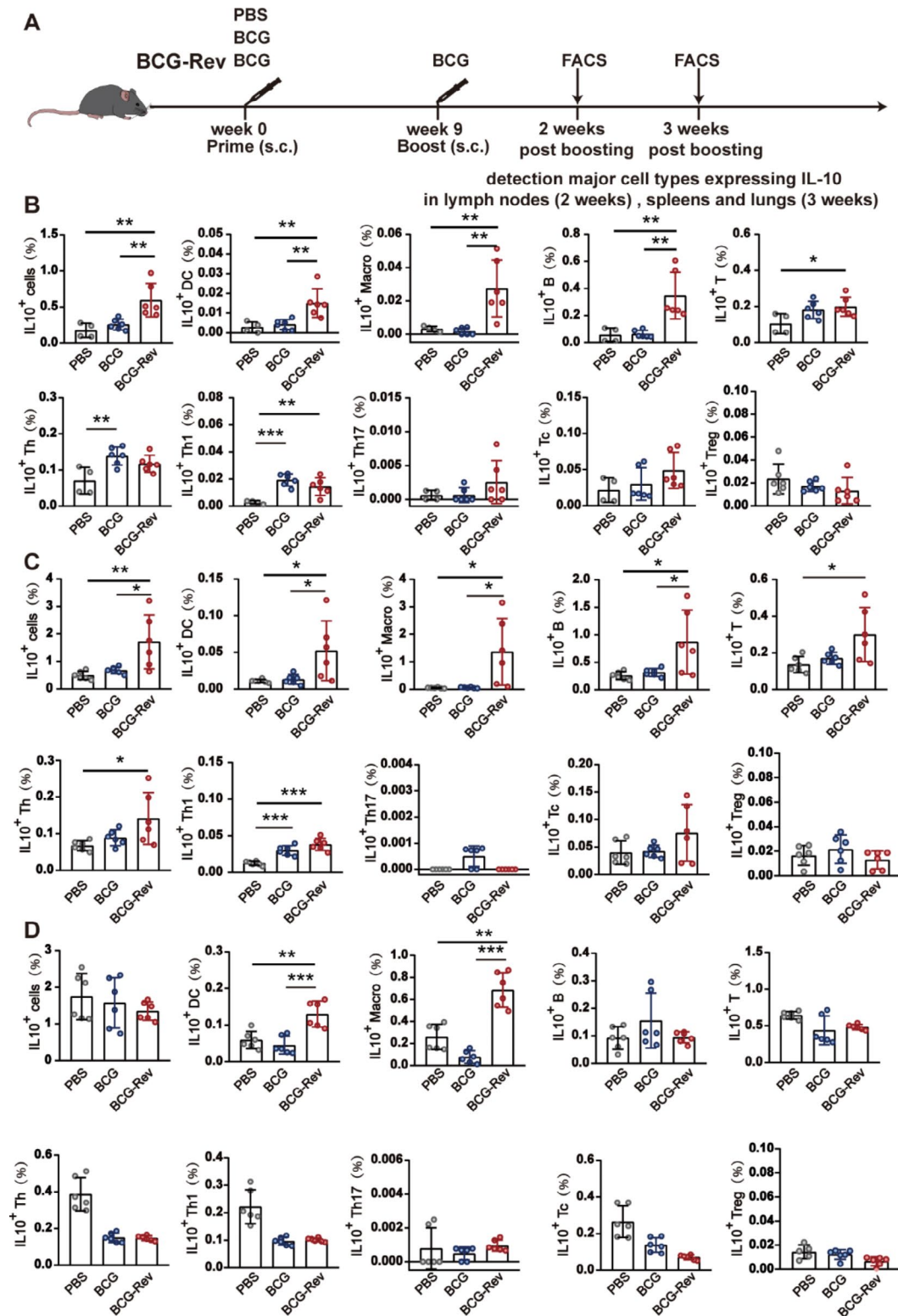


Fig. 4 Cell types expressing IL-10 in different organs ($n=6$). **(A)** Immunization and detection schedule. C57BL/6J mice received the BCG vaccine at week 0 and 9. Two or three weeks after the booster dose, ICS and FACS analyses were performed to evaluate the presence and abundance of IL-10-producing cells, including macrophages, dendritic cells (DCs), B cells, T cells, and T cell subsets such as helper T cells (Th), cytotoxic T cells (Tc), Th1 cells, Th17 cells, and regulatory T cells (Treg). The percentages of these IL-10⁺ cells in lymph nodes **(B)**, spleens **(C)**, and lungs **(D)** were compared across the three groups. Results are presented as mean \pm SD. * $P < 0.05$; ** $P < 0.01$; *** $P < 0.001$

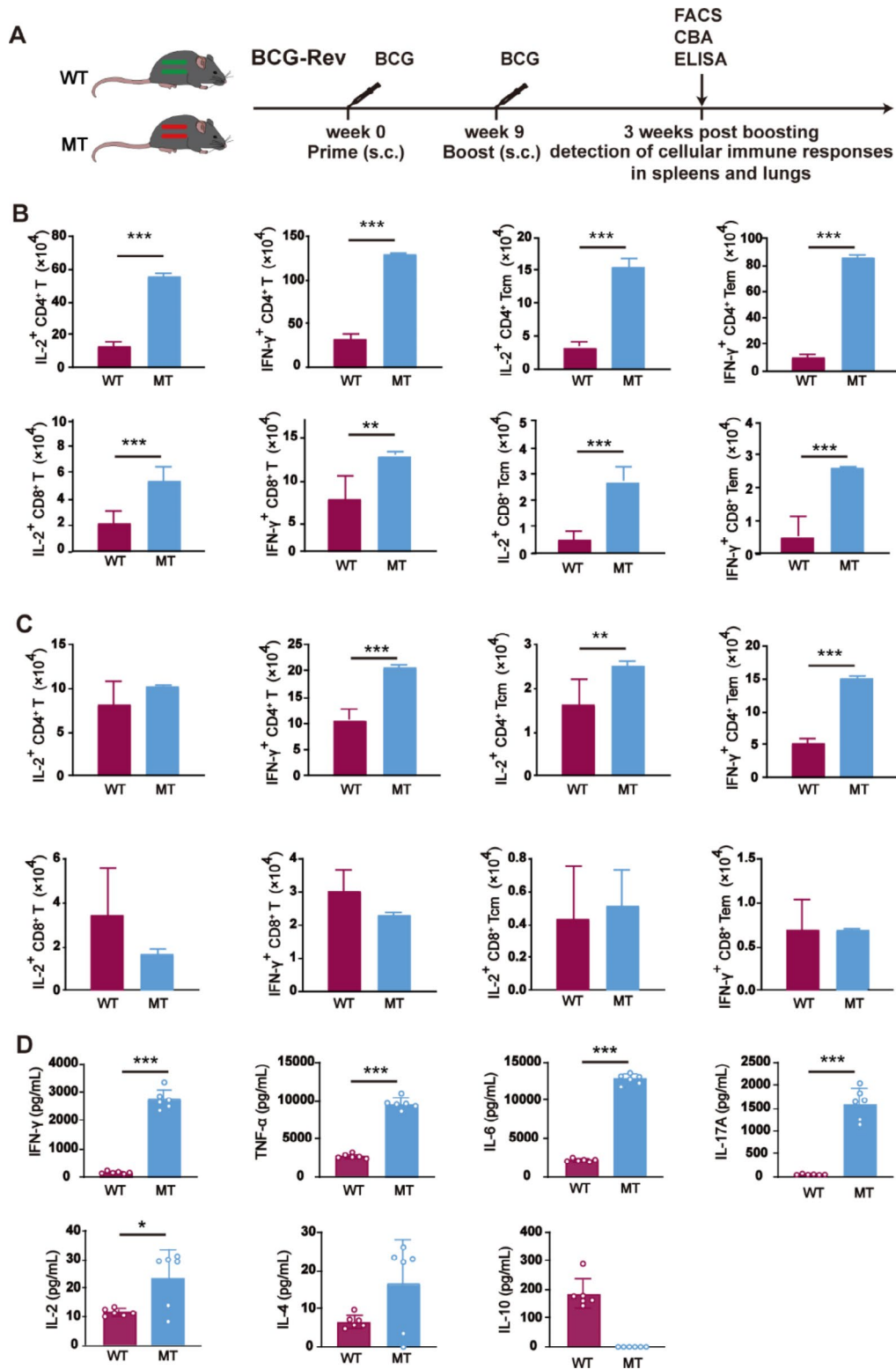


Fig. 5 Comparison of CMFO-specific T cell responses in the spleen and lung between BCG revaccinated WT mice and *IL-10*^{-/-} MT mice (n=6). **(A)** Immunization and detection schedule. Three weeks after the second dose, ICS and FACS analyses were employed to compare the absolute numbers of CMFO-specific IFN-γ⁺ and IL-2⁺ T cells, IL-2⁺ T_{CM} (CD62L^{hi} CD44^{hi}) cells, and IFN-γ⁺ T_{EM} (CD62L^{lo} CD44^{hi}) cells in the spleens **(B)** and lungs **(C)** of BCG-revaccinated C57BL/6J WT mice and *IL-10*^{-/-} mice. **(D)** CMFO-specific Th1, Th2, and Th17 cytokines, including IFN-γ, TNF-α, IL-6, IL-17, IL-2, IL-4, and IL-10, secreted into the supernatant of splenocytes, were also compared between the two groups. Results are expressed as mean ± SD (n=6). *P < 0.05; **P < 0.01; ***P < 0.001

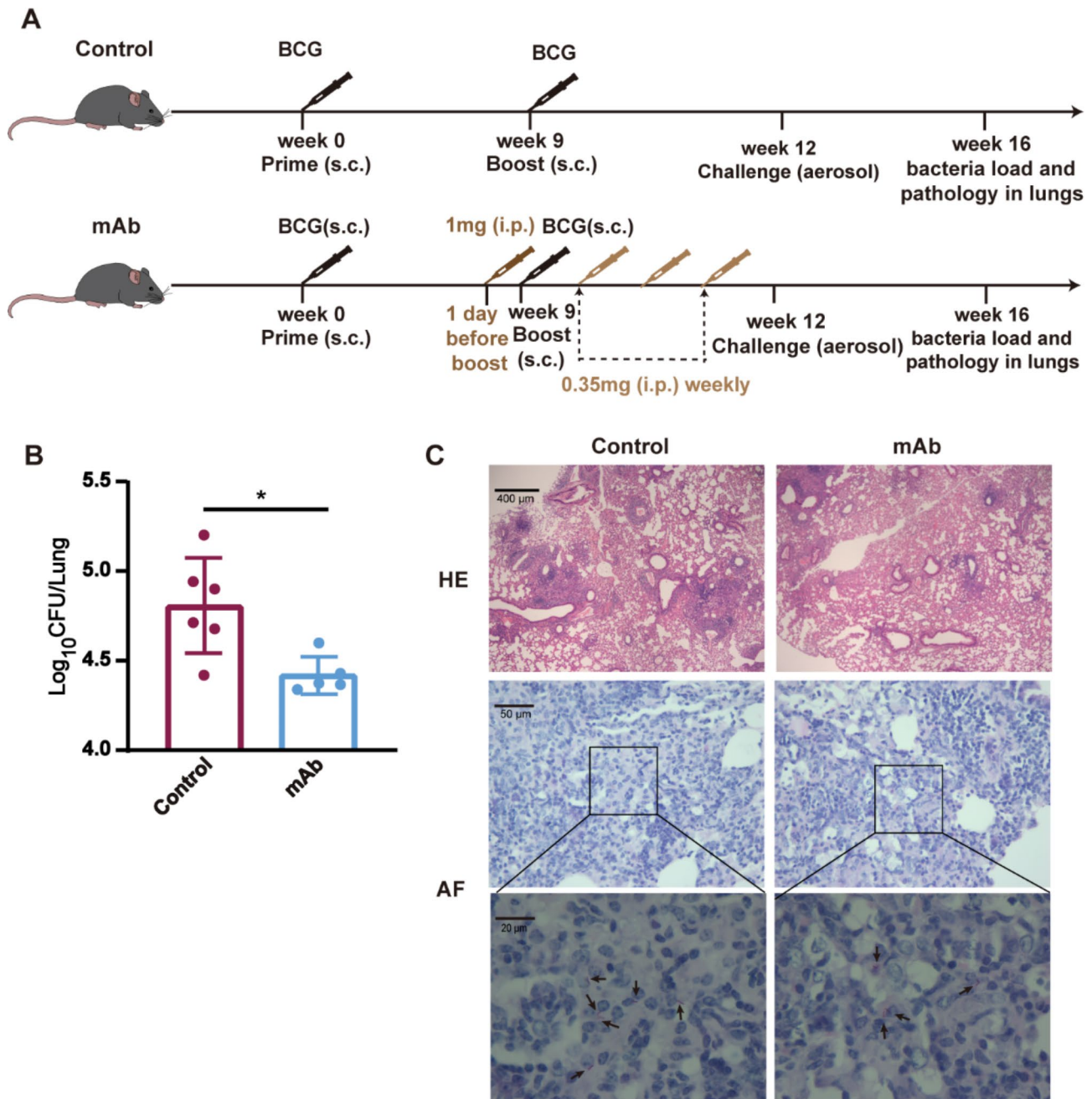


Fig. 6 Protective effect of inhibiting IL-10 signaling in BCG revaccinated mice against primary *M.tb* infection ($n=6$). **(A)** Immunization and detection schedule. Prior to the booster dose, BCG-primed C57BL/6J mice were administered anti-IL-10R mAb via intraperitoneal injection one day before the booster dose, followed by the second BCG vaccine dose and weekly mAb injections until the challenge with virulent *M. tuberculosis* H37Rv. After 12 weeks, the mice were infected with 300 CFU of *M. tuberculosis* H37Rv via aerosol exposure, and four weeks later, the lungs of mice from both groups were aseptically collected for evaluation of protective efficacy. **(B)** Comparison of bacterial loads in the lungs of both groups. **(C)** Lung pathological images, including HE and AF staining. Results are presented as mean \pm SEM ($n=6$). * $P < 0.05$; ** $P < 0.01$; *** $P < 0.001$

lungs (Fig. 6B) and showed reduced lung histopathological changes (Fig. 6C) compared to the untreated control group. Thus, blocking IL-10 signaling in BCG-revaccinated mice leads to enhanced protection against primary *M. tb* infection.

Discussion

Adolescents and adults currently represent the primary demographics affected by the TB epidemic. Given that infants typically receive BCG immunization, administering a booster during adolescence or adulthood—either with a homologous BCG vaccine or a heterologous

vaccine candidate—could be an effective strategy to protect adults from TB. However, suboptimal efficacy and an uncertain mechanism of action present significant obstacles to advancing this strategy for TB prevention in adults. Therefore, there is an urgent need to investigate the underlying mechanisms and develop essential technologies to overcome this barrier and facilitate the progress and implementation of an effective TB vaccine for adults. In this study, qRT-PCR was employed to assess differential cytokine expression in mice after BCG revaccination, revealing for the first time that IL-10, the only anti-inflammatory cytokine, is significantly upregulated in the lungs post-revaccination. Interestingly, this elevated IL-10 expression in the lungs was transient, persisting for 3–6 weeks after revaccination, irrespective of the interval between the prime and booster doses. IL-10 expression was also detected in the lymph nodes and spleen as early as the second week after the booster vaccination. In these tissues, IL-10 was primarily produced by antigen-presenting cells (APCs), including macrophages and dendritic cells. Inhibition of IL-10 signaling led to higher levels of antigen-specific CD4⁺ T cells and memory CD4⁺ T cell responses in the spleen and lungs of BCG-revaccinated mice, resulting in enhanced resistance to primary *M.tb* infection. These findings contribute to the formulation of a rational immunization strategy utilizing the BCG vaccine for TB prevention in adults.

Subcutaneous administration of the BCG vaccine results in the uptake of BCG by APCs in local lymph nodes, subsequently activating CD4⁺ T cells via the phagocytosis-lysosomal pathway and MHC class II molecules [24, 25]. Despite this, the immunological effects of repeated BCG immunizations have remained largely unrecognized until now. This study is the first to demonstrate that IL-10⁺ DCs and IL-10⁺ macrophages are induced in lymph nodes as early as the second week following the booster dose of the BCG vaccine, with these cells becoming significantly present in the spleen and lungs by the third week. Previous studies suggest that IL-10 may impair the host's ability to combat *M.tb* infection due to its inhibitory and anti-inflammatory properties. Furthermore, studies have shown that IL-10 compromises the protective efficacy of the BCG vaccine against *M.tb* infection after a single vaccination [26–30]. Specifically, IL-10 can suppress MHC II expression and impair the antigen-presenting ability of macrophages and DCs [31–34], thereby reducing TNF- α and IL-12 secretion and impeding the Th1 response. Additionally, IL-10⁺ Th1 cells and IL-10⁺ B cells were detected in the lymph nodes and spleen of mice revaccinated with the BCG vaccine. Evidence indicates that IL-10 prevents Th1 cell migration from lymph nodes to infection sites and reduces the production of antigen-specific T_{EM} cells and T_{CM} cells. Additionally, IL-10⁺ B cells may inhibit Th1

cell production and promote *M.tb* survival [35]. IL-10 has also been noted to contribute to compromised T cell function in individuals with TB [36]. Therefore, anti-IL-10R mAb has been extensively explored for the prevention and treatment of TB, yielding significant findings in various animal models [27–29, 37, 38]. For instance, after a single BCG vaccination, *IL-10*^{-/-} BALB/c mice exhibited increased IFN- γ ⁺ CD4⁺ T cells in the lungs [27]. Anti-IL-10R mAb inhibition of IL-10 signaling significantly increased memory CD4⁺ T cell numbers in CBA/J mice after a single BCG vaccination [37]. These results underscore the importance of *M.tb*-specific memory CD4⁺ T cell responses in TB protection, a concept well-established in the literature [36, 39]. It has been observed that inhibiting IL-10 signaling enhances CD4⁺ Th1 cell responses, leading to a marked improvement in the enduring protection conferred by a single BCG vaccination against *M.tb* infection [29]. Therefore, our study provides a rationale for elucidating why BCG revaccination fails to confer immunity against primary *M.tb* infection. BCG vaccine components, such as manLAM, can induce APCs to produce IL-10 [35, 40]. This phenomenon may be attributed to the intrinsic upregulation of IL-10 production following the second BCG dose, leading to a dampened memory CD4⁺ T cell response and diminished resistance to primary *M.tb* infection. Additionally, consistent with previous research [41, 42], BCG revaccinated mice exhibited a heightened level of IL-17. Numerous studies suggest that IL-17 might be involved in TB pathogenesis and progression; however, individuals who received a single BCG vaccination can induce IL-17 and Th17 cells [41–43], which have been linked to the BCG vaccine-induced protection against primary *M.tb* infection [19, 44]. Further investigation is needed to clarify the significance of elevated IL-17 expression in BCG-revaccinated mice and its impact on anti-TB immunity.

Although this study corroborates previous trials in Brazil and Malawi, which found no improvement in BCG efficacy against primary *M.tb* infection through revaccination [45–48], BCG revaccination has demonstrated benefits in preventing LTBI in mice and has been shown to be safe and immunogenic in individuals with positive interferon-gamma release assay (IGRA⁺) results [42]. Further research is needed to evaluate the efficacy and feasibility of incorporating BCG revaccination in individuals with LTBI, which could be achieved through LTBI screenings using IGRA methods in both infected and uninfected populations. Most importantly, assessing the levels of IL-10-expressing APC cells in lymph nodes, spleen, and lungs after BCG prime-boost immunization could help identify promising booster vaccine candidates, thereby advancing the development of adult TB vaccines.

Abbreviations

APC	Antigen presenting cell
BCG	Bacillus Calmette-Guérin
CBA	Cytometric Bead Array
CFU	Colony-forming unit
FACS	Fluorescence activated cell sorting
ICS	Intracellular cytokine staining
LTBI	Latent tuberculosis infection
MHC	Major histocompatibility complex
MT	Mutant-type
<i>M.tb</i>	<i>Mycobacterium tuberculosis</i>
PCR	Polymerase Chain Reaction
qRT-PCR	Quantitative real time PCR
TB	Tuberculosis
T _{CM}	Central memory T cell
T _{EM}	Effector memory T cell
Th	T helper cells
WT	Wild-type

Supplementary Information

The online version contains supplementary material available at <https://doi.org/10.1186/s12967-024-05683-w>.

Supplementary Material 1

Acknowledgements

This work was supported by grants from the Natural Science Foundation of China (No. 81971909) and the National Key R & D project of China (2022YFA1303503).

Author contributions

Fan X designed the study. Lei Q, Yao ZJ, Fu H, Zhou ZJ and Lin XS performed experiments and collected the data. Lei Q, Yao ZJ, Wang YQ, Yuan Y, Ouyang Q, Xu XY, Cao JG and Gan MZ analyzed the data. Lei Q and Fu H draw the figures and wrote the original manuscript, and Fan X revised the manuscript.

Data availability

All data are contained in manuscripts or supplementary information files provided.

Declarations

Conflict of interest

The authors declare no conflicts of interest.

Author details

¹Department of Pathogen Biology, School of Basic Medicine, Tongji Medical College and State Key Laboratory for Diagnosis and Treatment of Severe Zoonotic Infectious Diseases, Hubei Key Laboratory of Drug Target Research and Pharmacodynamic Evaluation, Huazhong University of Science and Technology, Wuhan, China

²Department of Infectious Disease, Leiden University Medical Center, Leiden 2333 ZA, The Netherlands

³Department of Laboratory Medicine, Wuhan No. 1 Hospital, Tongji Medical College, Huazhong University of Science and Technology, Wuhan, China

⁴Department of Pediatrics, Union Hospital, Tongji Medical College, Huazhong University of Science and Technology, Wuhan, China

Received: 9 July 2024 / Accepted: 4 September 2024

Published online: 04 December 2024

References

- Lange C, et al. 100 years of *Mycobacterium bovis* Bacille Calmette-Guérin. *Lancet Infect Dis*. 2022;22. [https://doi.org/10.1016/S1473-3099\(21\)00403-5](https://doi.org/10.1016/S1473-3099(21)00403-5).
- Roy P, et al. Potential effect of age of BCG vaccination on global paediatric tuberculosis mortality: a modelling study. *Lancet Glob Health*. 2019;7:e1655–63. [https://doi.org/10.1016/S2214-109X\(19\)30444-9](https://doi.org/10.1016/S2214-109X(19)30444-9).
- Zwerling A, et al. The BCG World Atlas: a database of global BCG vaccination policies and practices. *PLoS Med*. 2011;8:e1001012. <https://doi.org/10.1371/journal.pmed.1001012>.
- Lancione S, Alvarez JV, Alsdurf H, Pai M, Zwerling AA. Tracking changes in national BCG vaccination policies and practices using the BCG World Atlas. *BMJ Glob Health*. 2022;7. <https://doi.org/10.1136/bmjgh-2021-007462>.
- Moutinho S. Tuberculosis is the oldest pandemic, and poverty makes it continue. *Nature*. 2022;605:S16–20. <https://doi.org/10.1038/d41586-022-01348-0>.
- Global tuberculosis report 2022*, <https://www.who.int/teams/global-tuberculosis-programme/tb-reports> (2022).
- Schrager LK, et al. WHO preferred product characteristics for new vaccines against tuberculosis. *Lancet Infect Dis*. 2018;18:828–9. [https://doi.org/10.1016/S1473-3099\(18\)30421-3](https://doi.org/10.1016/S1473-3099(18)30421-3).
- Hatherill M, Cobelens F. Infant. BCG vaccination is beneficial, but not sufficient. *Lancet Glob Health*. 2022;10:e1220–1. [https://doi.org/10.1016/S2214-109X\(22\)00325-4](https://doi.org/10.1016/S2214-109X(22)00325-4).
- Marais BJ, et al. Interrupted BCG vaccination is a major threat to global child health. *Lancet Respir Med*. 2016;4:251–3. [https://doi.org/10.1016/S2213-2600\(16\)00099-0](https://doi.org/10.1016/S2213-2600(16)00099-0).
- WHO statement on BCG revaccination for the prevention of tuberculosis. *Bull World Health Organ*. 1995;73:805–6.
- BCG vaccines. WHO position paper – February 2018. *Wkly Epidemiol Rec*. 2018;93:73–96.
- Nieuwenhuizen NE, Kaufmann SHE. Next-generation vaccines based on Bacille Calmette-Guérin. *Front Immunol*. 2018;9:121. <https://doi.org/10.3389/fimmu.2018.00121>.
- Brennan MJ, et al. Preclinical evidence for implementing a prime-boost vaccine strategy for tuberculosis. *Vaccine*. 2012;30:2811–23. <https://doi.org/10.1016/j.vaccine.2012.02.036>.
- Darrah, P. A. et al. Boosting BCG with proteins or rAd5 does not enhance protection against tuberculosis in rhesus macaques. *NPJ Vaccines*. 2019;4:21. <https://doi.org/10.1038/s41541-019-0113-9>.
- Nemes E, et al. Prevention of *M. Tuberculosis* infection with H4:IC31 vaccine or BCG Revaccination. *N Engl J Med*. 2018;379:138–49. <https://doi.org/10.1056/NEJMoa1714021>.
- Wu Y, et al. Heterologous Boost following *Mycobacterium bovis* BCG reduces the late persistent, rather than the early stage of Intranasal Tuberculosis Challenge Infection. *Front Immunol*. 2018;9:2439. <https://doi.org/10.3389/fimmu.2018.02439>.
- Ma J, et al. A multistage subunit vaccine effectively protects mice against Primary Progressive Tuberculosis, latency and reactivation. *EBioMedicine*. 2017;22:143–54. <https://doi.org/10.1016/j.ebiom.2017.07.005>.
- North RJ, Jung Y-J. Immunity to tuberculosis. *Annu Rev Immunol*. 2004;22:599–623.
- Lyadova IV, Pantelev AV. Th1 and Th17 Cells in Tuberculosis: Protection, Pathology, and Biomarkers. *Mediators Inflamm* 2015, 854507, <https://doi.org/10.1155/2015/854507> (2015).
- Zeng G, Zhang G, Chen X. Th1 cytokines, true functional signatures for protective immunity against TB? *Cell Mol Immunol*. 2018;15:206–15. <https://doi.org/10.1038/cmi.2017.113>.
- Hao L, et al. Combinational PRR agonists in liposomal adjuvant enhances immunogenicity and protective efficacy in a tuberculosis subunit vaccine. *Front Immunol*. 2020;11:575504. <https://doi.org/10.3389/fimmu.2020.575504>.
- Ullah N et al. Differential Immunogenicity and Protective Efficacy Elicited by MTO- and DMT-Adjuvanted CMFO Subunit Vaccines against *Mycobacterium tuberculosis* Infection. *J Immunol Res* 2020, 2083793, <https://doi.org/10.1155/2020/2083793> (2020).
- Liu C, et al. Cytokines: from clinical significance to quantification. *Adv Sci (Weinh)*. 2021;8:e2004433. <https://doi.org/10.1002/advs.202004433>.
- Moliva JI, Turner J, Torrelles JB. Immune responses to Bacillus Calmette-Guérin vaccination: why do they fail to protect against *Mycobacterium tuberculosis*? *Front Immunol*. 2017;8:407. <https://doi.org/10.3389/fimmu.2017.00407>.
- Covián C, et al. BCG-Induced Cross-protection and Development of trained immunity: implication for Vaccine Design. *Front Immunol*. 2019;10:2806. <https://doi.org/10.3389/fimmu.2019.02806>.
- Redford PS, Murray PJ, O'Garra A. The role of IL-10 in immune regulation during *M. Tuberculosis* infection. *Mucosal Immunol*. 2011;4:261–70. <https://doi.org/10.1038/mi.2011.7>.

27. Redford PS, et al. Enhanced protection to *Mycobacterium tuberculosis* infection in IL-10-deficient mice is accompanied by early and enhanced Th1 responses in the lung. *Eur J Immunol*. 2010;40:2200–10. <https://doi.org/10.1002/eji.201040433>.
28. Silva RA, Pais TF, Appelberg R. Blocking the receptor for IL-10 improves anti-mycobacterial chemotherapy and vaccination. *J Immunol*. 2001;167:1535–41.
29. Pitt JM, et al. Blockade of IL-10 signaling during bacillus Calmette-Guérin vaccination enhances and sustains Th1, Th17, and innate lymphoid IFN- γ and IL-17 responses and increases protection to *Mycobacterium tuberculosis* infection. *J Immunol*. 2012;189:4079–87. <https://doi.org/10.4049/jimmunol.1201061>.
30. Xu H, et al. IL-10 dampens the Th1 and Tc activation through modulating DC functions in BCG Vaccination. *Mediators Inflamm*. 2019;2019(8616154). <https://doi.org/10.1155/2019/8616154>.
31. Schreiber T, et al. Autocrine IL-10 induces hallmarks of alternative activation in macrophages and suppresses antituberculosis effector mechanisms without compromising T cell immunity. *J Immunol*. 2009;183:1301–12. <https://doi.org/10.4049/jimmunol.0803567>.
32. Chatterjee S, et al. Mycobacteria induce TPL-2 mediated IL-10 in IL-4-generated alternatively activated macrophages. *PLoS ONE*. 2017;12:e0179701. <https://doi.org/10.1371/journal.pone.0179701>.
33. Verma R, et al. A network map of Interleukin-10 signaling pathway. *J Cell Commun Signal*. 2016;10:61–7. <https://doi.org/10.1007/s12079-015-0302-x>.
34. Ferreira CM, et al. Early IL-10 promotes vasculature-associated CD4+T cells unable to control *Mycobacterium tuberculosis* infection. *JCI Insight*. 2021;6. <https://doi.org/10.1172/jci.insight.150060>.
35. Yuan C, et al. Mycobacterium tuberculosis Mannose-Capped Lipoarabinomannan induces IL-10-Producing B cells and hinders CD4+Th1 immunity. *iScience*. 2019;11:13–30. <https://doi.org/10.1016/j.isci.2018.11.039>.
36. Harling K, et al. Constitutive STAT3 phosphorylation and IL-6/IL-10 co-expression are associated with impaired T-cell function in tuberculosis patients. *Cell Mol Immunol*. 2019;16:275–87. <https://doi.org/10.1038/cmi.2018.5>.
37. Dwivedi V, et al. IL-10 receptor blockade delivered simultaneously with Bacillus Calmette-Guérin vaccination sustains long-term protection against *Mycobacterium tuberculosis* infection in mice. *J Immunol*. 2022;208:1406–16. <https://doi.org/10.4049/jimmunol.2100900>.
38. Wong EA, et al. IL-10 impairs local Immune response in Lung Granulomas and Lymph Nodes during early *Mycobacterium tuberculosis* infection. *J Immunol*. 2020;204:644–59. <https://doi.org/10.4049/jimmunol.1901211>.
39. Foster M, et al. BCG-induced protection against *Mycobacterium tuberculosis* infection: evidence, mechanisms, and implications for next-generation vaccines. *Immunol Rev*. 2021;301:122–44. <https://doi.org/10.1111/imr.12965>.
40. Yuan C-H, et al. Mannose-capped lipoarabinomannan-induced B10 cells decrease severity of dextran sodium sulphate-induced inflammatory bowel disease in mice. *Scand J Immunol*. 2020;91:e12843. <https://doi.org/10.1111/sji.12843>.
41. Cruz A, et al. Pathological role of interleukin 17 in mice subjected to repeated BCG vaccination after infection with *Mycobacterium tuberculosis*. *J Exp Med*. 2010;207:1609–16. <https://doi.org/10.1084/jem.20100265>.
42. Rakshit S, et al. BCG revaccination boosts adaptive polyfunctional Th1/Th17 and innate effectors in IGRA+ and IGRA- Indian adults. *JCI Insight*. 2019;4. <https://doi.org/10.1172/jci.insight.130540>.
43. Scriba TJ, et al. Sequential inflammatory processes define human progression from *M. Tuberculosis* infection to tuberculosis disease. *PLoS Pathog*. 2017;13:e1006687. <https://doi.org/10.1371/journal.ppat.1006687>.
44. Shen H, Chen ZW. The crucial roles of Th17-related cytokines/signal pathways in *M. Tuberculosis* infection. *Cell Mol Immunol*. 2018;15:216–25. <https://doi.org/10.1038/cmi.2017.128>.
45. Randomised controlled trial of single BCG, Repeated BCG, or combined BCG and killed *Mycobacterium leprae* vaccine for prevention of leprosy and tuberculosis in Malawi. Karonga Prevention Trial Group. *Lancet*. 1996;348:17–24.
46. Glynn JR, et al. The effect of BCG revaccination on all-cause mortality beyond infancy: 30-year follow-up of a population-based, double-blind, randomised placebo-controlled trial in Malawi. *Lancet Infect Dis*. 2021;21:1590–7. [https://doi.org/10.1016/s1473-3099\(20\)30994-4](https://doi.org/10.1016/s1473-3099(20)30994-4).
47. Glynn JR, et al. BCG re-vaccination in Malawi: 30-year follow-up of a large, randomised, double-blind, placebo-controlled trial. *Lancet Glob Health*. 2021;9:e1451–9. [https://doi.org/10.1016/S2214-109X\(21\)00309-0](https://doi.org/10.1016/S2214-109X(21)00309-0).
48. Barreto ML, et al. Evidence of an effect of BCG revaccination on incidence of tuberculosis in school-aged children in Brazil: second report of the BCG-REVAC cluster-randomised trial. *Vaccine*. 2011;29:4875–7. <https://doi.org/10.1016/j.vaccine.2011.05.023>.

Publisher's note

Springer Nature remains neutral with regard to jurisdictional claims in published maps and institutional affiliations.